Activation of Nuclear Factor κB by Polyamines in Breast Cancer Cells†

Neha Shah,[‡,§] Thresia Thomas,[||,⊥,○] Akira Shirahata,[#] Leonard H. Sigal,[‡,⊗] and T. J. Thomas*[,‡,§,○]

Departments of Medicine, Environmental and Community Medicine, Molecular Genetics and Microbiology and Pediatrics, the Environmental and Occupational Health Sciences Institute, and The Cancer Institute of New Jersey, University of Medicine and Dentistry of New Jersey−Robert Wood Johnson Medical School, New Brunswick, New Jersey 08903, Nutritional Sciences Graduate Program, Rutgers−The State University of New Jersey, New Brunswick, New Jersey 08903, and the Faculty of Pharmaceutical Sciences, Josai University, Sakado, Saitama 350-02, Japan

Received June 8, 1999; Revised Manuscript Received September 7, 1999

ABSTRACT: Polyamines—putrescine, spermidine, and spermine—are involved in the growth of breast cancer cells. A possible target of polyamine action is at the site of interaction of transcription factors with their response elements. NF-κB is a member of the rel family of transcription factors that regulate transcription of genes in the proliferative/anti-apoptotic pathways. We performed electrophoretic mobility shift assays to study the role of polyamines in NF-κB binding to NF-κB response elements (NREs), the consensus sequence of which is GGGGAATTCCCC. Using cellular extract from MCF-7 breast cancer cells, we found very little binding of NF-κB to NRE in the absence of polyamines. Addition of 1 mM spermidine or spermine caused a 4- and 6-fold increase in NF-κB−NRE binding, respectively. Putrescine induced a 2-fold increase in the binding at 2 mM concentration. Using antibody supershift assays, we identified the p50 subunit of NF-κB to be a major component in NF-κB−NRE complex formation in the presence of polyamines. However, the decreased intensity of the band corresponding to NF-κB−NRE complex in the presence of anti-p65, c-rel, relB and p52 antibodies suggested the participation of these subunits also. Spermine also stimulated NF-κB−NRE binding using cellular extracts from other breast cancer cell lines and a normal breast epithelial cell line. A differential effect of spermine analogues on NF-κB−NRE binding was observed, with spermine exerting the maximal effect. CD spectra of NRE containing oligonucleotides was asymmetric and distinct from that of a typical B-DNA CD spectrum. A concentration-dependent increase in T_m of the duplex NRE was seen in the presence of polyamines. In transient transfection experiments using an NF-κB driven secreted alkaline phosphatase (SEAP) reporter, spermine induced NF-κB activity by ∼2-fold as compared to controls. Spermine induced activation of NF-κB was also confirmed using an NF-κB−EGFP (enhanced green fluorescent protein) vector in transient transfections in which expression of the green fluorescent protein was visualized by fluorescence microscopy. These data show a gene regulatory function of polyamines involving enhanced binding of NF-κB to NRE and a possible mechanism for the action of polyamines in breast cancer cell proliferation.

The natural polyamines, putrescine, spermidine, and spermine, are ubiquitous cellular polycations with multiple functions in cell growth and differentiation (*1, 2*). Polyamine levels are generally in the millimolar range and are highly regulated by various biosynthetic and metabolizing enzymes, and polyamines themselves play a major role in determining their rates of synthesis and degradation (*1*). In cancer cells, polyamine biosynthetic activity and polyamine levels are significantly higher than that in normal cells (*3*−*6*). Elevated polyamine levels are thought to be required for both the development and/or maintenance of the neoplastic phenotype (*7, 8*), although their mechanism of action at the molecular level is not well-defined. Use of polyamine biosynthesis inhibitors has shown that polyamine biosynthesis is an obligatory step in both the initiation and maintenance of cell proliferation (*6*−*8*). These studies suggest the potential of targeting the polyamine pathway as a strategy for cancer therapy. The interaction of polyamines with transcription factors and their cognate sequences provides a pathway for their ability to regulate gene expression (9,*10*).

The rel family of transcription factors includes the p50, p52, p65 (relA), rel-B, and c-rel proteins that form homo-

† This work was supported, in part, by research grant nos. CA42439 and CA73058 from the National Cancer Institute (T. J. T. and T. T.), Molecular Biophysics Training Grant T32 GM08319 from the NIH (Wilma Olson), Outstanding Breast Cancer Research Grants from the New Jersey State Commission on Cancer Research (T. J. T. and T. T.), and a Grant-in-Aid for Scientific Research from the Ministry of Education, Science, and Culture, Japan (A. S.).

* Corresponding author at the Clinical Academic Building, Room 7090, UMDNJ−Robert Wood Johnson Medical School, 125 Paterson Street, New Brunswick, NJ 08903. Telephone: 732-235-8460. Fax: 732-235-8473. E-mail: thomastj@UMDNJ.edu.

‡ Department of Medicine, Robert Wood Johnson Medical School.

§ Nutritional Sciences Graduate Program, Rutgers−The State University of New Jersey.

|| Environmental and Occupational Health Sciences Institute, Robert Wood Johnson Medical School.

○ The Cancer Institute of New Jersey, Robert Wood Johnson Medical School.

Faculty of Pharmaceutical Sciences, Josai University.

⊗ Department of Molecular Genetics and Microbiology and Pediatrics, Robert Wood Johnson Medical School.

10.1021/bi991291v CCC: $18.00
Published on Web 10/23/1999

Put:	$NH_2(CH_2)_4NH_2$
Spd:	$NH_2(CH_2)_3NH(CH_2)_4NH_2$
Spm:	$NH_2(CH_2)_3NH(CH_2)_4NH(CH_2)_3NH_2$
3-2:	$NH_2(CH_2)_3NH(CH_2)_2NH_2$
3-3:	$NH_2(CH_2)_3NH(CH_2)_3NH_2$
3-5:	$NH_2(CH_2)_3NH(CH_2)_5NH_2$
3-6:	$NH_2(CH_2)_3NH(CH_2)_6NH_2$
3-7:	$NH_2(CH_2)_3NH(CH_2)_7NH_2$
3-8:	$NH_2(CH_2)_3NH(CH_2)_8NH_2$
3-2-3:	$NH_2(CH_2)_3NH(CH_2)_2NH(CH_2)_3NH_2$
3-3-3:	$NH_2(CH_2)_3NH(CH_2)_3NH(CH_2)_3NH_2$
3-5-3:	$NH_2(CH_2)_3NH(CH_2)_5NH(CH_2)_3NH_2$
3-6-3:	$NH_2(CH_2)_3NH(CH_2)_6NH(CH_2)_3NH_2$
3-7-3:	$NH_2(CH_2)_3NH(CH_2)_7NH(CH_2)_3NH_2$
3-8-3:	$NH_2(CH_2)_3NH(CH_2)_8NH(CH_2)_3NH_2$
3-9-3:	$NH_2(CH_2)_3NH(CH_2)_9NH(CH_2)_3NH_2$
BE-3-3-3:	$C_2H_5NH(CH_2)_3NH(CH_2)_3NH(CH_2)_3NHC_2H_5$
BE-3-4-3:	$C_2H_5NH(CH_2)_3NH(CH_2)_4NH(CH_2)_3NHC_2H_5$
BE-3-7-3:	$C_2H_5NH(CH_2)_3NH(CH_2)_7NH(CH_2)_3NHC_2H_5$

FIGURE 1: Chemical structures of polyamines and their analogues used in this study.

or heterodimers of various combinations of these proteins (*11*). Each subunit has a RHD of about 300 amino acids in length, which determines DNA binding, dimerization with identical or other members of the family, nuclear translocation, and interaction with inhibitor proteins, IκBs. Classic NF-κB is a p50/p65 heterodimer and typically resides in the cytoplasm in an inactive form, bound by IκBs (*11*). NF-κB is activated by a variety of stimuli, such as oxidative stress, cytokines, and drugs used in anticancer treatment (*12*, *13*). Upon stimulation, IκB undergoes phosphorylation and subsequent degradation, resulting in the release of NF-κB, which translocates into the nucleus and binds to NRE sequences present in the upstream regulatory regions of several genes, including those involved in stimulating cell proliferation and preventing apoptosis (*11*−*14*). An increase in cellular polyamine levels is also associated with increased cell proliferation (*3*−*8*) and decreased apoptosis (*15*).

Aberrant nuclear expression of NF-κB has been associated with human breast cancer as well as carcinogen-induced rat mammary tumorigenesis (*16*). Direct inhibition of NF-κB activity in breast tumor cell lines with high levels of nuclear NF-κB activity, induced apoptosis (*16*). Nakshatri et al. (*17*) have recently shown much higher constitutive binding of NF-κB to its response element in ER-negative breast cancer cell lines as well as ER-negative primary breast tumors. There are several reports supporting the involvement of NF-κB in the inhibition of the apoptotic response induced by TNF-α, ionizing radiation or chemotherapeutic agents, suggesting that NF-κB may play an anti-apoptotic role in many systems (*18*). Thus, inhibition of NF-κB activation is an effective molecular approach to increasing apoptosis sensitivity of cancer cells. To understand the cellular regulatory factors involved in NF-κB activation in breast cancer cells, we investigated the ionic and structural specificity effects of polyamines on NF-κB−NRE interactions.

Synthetic polyamine analogues, such as bis(ethyl)norspermine (BE-3-3-3, please see Figure 1 for chemical structures) are known to have antitumor activity (*8*). The cell growth inhibitory activity of these compounds may, in part, be due to their inability to facilitate gene regulatory protein−DNA interactions, such as the binding of NF-κB with its response elements. Therefore, we conducted a series of experiments to elucidate the structure−activity relationship of polyamines in the activation of NF-κB by polyamines. Our results showed that spermine is the most effective natural polyamine in facilitating NF-κB−NRE interactions. Polyamine analogues are less effective than the natural polyamines in facilitating these interactions, suggesting that the structural geometry of spermine is more conducive to NF-κB binding to NRE. These differential effects of polyamines might be useful in designing polyamine analogues to inhibit breast cancer cell growth.

MATERIALS AND METHODS

Chemicals and Reagents. Putrescine·2HCl, spermidine·3HCl, and spermine·4HCl were purchased from Sigma Chemical Co. (St. Louis, MO). The structural homologues of spermidine, 1,6-diamino-3-azahexane (3-2), 1,7-diamino-4-azaheptane (3-3), 1,9-diamino-4- azanonane (3-5), 1,10-diamino-4-azadecane (3-6), 1,11-diamino-4-azaundecane (3-7), and 1,12-diamino-4-azadodecane (3-8), and spermine, 1,10-diamino-4,7-diazadecane (3-2-3), 1,11-diamino-4,8-diazaundecane (3-3-3, norspermine), 1,13-diamino-4,10- diazatridecane (3-5-3), 1,14-diamino-4,11-diazatetradecane (3-6-3), 1,15-diamino- 4,11-diazapentadecane (3-7-3), 1,16-diamino-4,13-diazahexadecane (3-8-3), 1,17-diamino-4,13-diazaheptadecane (3-9-3), were synthesized as previously described (*19*−*21*). The bis(ethyl)polyamine analogues, 3,7,-12,16-tetrazaoctadecane (BE-3-4-3 or BE-Spm), 3,7,11,15-tetrazaheptadecane (BE-3-3-3), and 3,7,15,19-tetrazahenicosane (BE-3-7-3) were also synthesized according to previously described methods (*22*, *23*). The structures and purity of all polyamines were confirmed by elemental analysis, NMR, HPLC, and mass spectrometry. Figure 1 shows the chemical structures of the natural and synthetic polyamines used in this study. Polyamine solutions were made in double distilled water, and appropriate dilutions were made prior to use. Purified human recombinant p50 was purchased from Promega (Madison, WI). Fetal bovine serum, DMEM, Phenol-free F12−DMEM, IMEM, and McCoy's 5A modified medium were purchased from Sigma (St. Louis,

[1] Abbreviations: CD, circular dichroism; COX-2, cyclooxygenase-2; DFMO, D,L-α-difluoromethylornithine; DMEM, Dulbecco's modified Eagle's medium; EGF, epidermal growth factor; GFP, green fluorescent protein; EGFP, enhanced green fluorescent protein; EMSA, electrophoretic mobility shift assay; iNOS, inducible nitric oxide synthase; IκB, inhibitor of NF-κB IMEM; improved minimum essential medium; NO, nitric oxide; NF-κB, nuclear factor κB; NRE, NF-κB response element, ODC, ornithine decarboxylase; RHD, rel homology domain; SAMDC, *S*-adenosyl methionine decarboxylase; SEAP, secreted alkaline phosphatase; SSAT, spermidine-spermine acetyl transferase; Tm, melting temperature; TNF, tumor necrosis factor.

MO). Poly(dI−dC)·poly(dI−dC) was purchased from Pharmacia (Piscataway, NJ). Antibodies to the rel proteins p50, p65, p52, rel-B, and c-rel, were purchased from Santa Cruz Biotechnology (Santa Cruz, California). A second anti-p65 antibody was purchased from Upstate Biotechnology (Lake Placid, New York).

The pNFκB−SEAP, pβ-gal-control, and pNF-κB-d2EGFP vectors were purchased from Clontech Laboratories (Palo Alto, CA). Calcium phosphate mammalian transfection kit, Great Escape SEAP chemiluminescence detection kit, and luminescent β-galactosidase detection kits were also purchased from Clontech Laboratories.

Oligonucleotides. HPLC purified oligonucleotides were purchased from Oligos Etc., Inc. (Wilsonville, OR). A 32-base oligonucleotide containing the consensus NF-κB sequence (NRE-1) was used for EMSA, CD, and T_m studies. A 29-base complementary sequence was chosen to allow for efficient end-labeling. A control oligonucleotide (c-NRE) of the same base composition as NRE-1, but with scrambled sequence, was also used for CD and T_m studies. A mutated NRE-1 (*m*-NRE) with a two base rearrangement in the consensus sequence was used in EMSA for determining sequence specificity of NF-κB binding. Other NRE containing sequences present in the κ light chain enhancer of B cells (NRE-2), and in the promoter region of the iNOS gene (NRE-3), and COX-2 gene (NRE-4) were also used for EMSA. The oligonucleotides were dissolved in a buffer containing 10 mM Tris·HCl (pH 7.5) and 50 mM NaCl, and dialyzed three times against the same buffer before use. Base sequences of the top strand of NRE oligonucleotides used are as follows:

NRE-1: 5′ TTGGCAACGGCA*GGGGAATTCCCC*T-CTCCTTA 3′

NRE-2: 5′ GCAAGTTGA*GGGGACTTTCCC*AGGC 3′

NRE-3: 5′ TTGGCAACGGCA*GGGATTTTCC*T-CTCCTTA 3′

NRE-4: 5′ TTGGCAACGGCA*GGGGATTCCC*T-CTCCTTA 3′

c-NRE: 5′ TCCTACGGCGGCCGTAGCAATCAC-GTCGTTTA 3′

m-NRE-1: 5′ TTGGCAACGGCA-*GGTTAAGGCCCC*TCTCCTTA 3′

Cell Culture and Treatments. We used the following cell lines for this study: (i) ER-positive MCF-7, (ii) ER-transfected MCF-10AE^{wt5} (*24*), (iii) ER-negative MDA-MB-231, (iv) ER-negative MDA-MB-468, (v) ER-negative SK−BR-3, and (vi) normal breast epithelial cell line, MCF-10A. All cell lines except MCF-10AE^{wt5} were obtained from the American Type Culture Collection (Rockville, MD). MCF-10AE^{wt5} cell line was obtained by transfecting a wild-type ER cDNA containing plasmid, hEGO in pSG5 (obtained from Professor P. Chambon) in MCF-10A (*24*). MCF-7 cells were maintained in DMEM with 100 μg/mL penicillin, 100 μg/mL streptomycin, 40 μg/mL gentamycin, 2 μg/mL insulin, 0.4 mM sodium pyruvate, 10 mM nonessential amino acids, 4 mM L-glutamine, and 10% fetal bovine serum. MCF-10A and MCF-10AE^{wt5} cells were maintained in phenol-free F12−DMEM with 100 μg/mL penicillin, 100 μg/mL streptomycin, 40 μg/mL gentamycin, 4 mM L-glutamine, 10 μg/mL insulin, 2 ng/mL EGF, 100 ng/mL cholera toxin, 0.5 μg/mL hydrocortisone, and 5% DCC-treated fetal bovine serum. In addition to the above-mentioned components, the MCF-10AE^{wt5} cells also received 1 mM G418. MDA-MB-231 and MDA-MB-468 cells were maintained in IMEM with 100 μg/mL penicillin, 100 μg/mL streptomycin, 40 μg/mL gentamycin, 0.4 mM sodium pyruvate, 4 mM L-glutamine, and 10% fetal bovine serum. SK−BR-3 cells were maintained in McCoy's 5A modified medium with 3 mM L-glutamine, and 10% fetal bovine serum. For spermine treatment experiments, MCF-7 cells at 60−70% confluence were treated with the indicated concentrations of spermine and 1 mM aminoguanidine for 6 h. Aminoguanidine was added to cells along with spermine to inhibit the action of polyamine oxidase. For polyamine assay, 2×10^6 cells were plated in 60 mm dishes and allowed to adhere for 24 h before treatment with spermine.

Preparation of Cellular Extract. For EMSA, cells were harvested by mild trypsinization, centrifuged, and the cell pellets were sonicated at 4 °C in 10 volumes of a buffer containing 50 mM Tris·HCl, 1.5 mM EDTA, 50 mM NaCl, 400 mM KCl, 10% glycerol (TEG buffer with KCl, pH 7.4) and 1 mM β-mercaptoethanol using a Branson 450 sonifier, three times for 5 s each (*9*). Cellular lysate was centrifuged at 105 000*g* for 45 min on a glycerol cushion using a Beckman Optima LE-80K ultracentrifuge. The supernate was aliquoted and stored at −70 °C until used for experiments. For polyamine assay, cell pellets were sonicated in 300 μL of 8% sulfosalysilic acid and incubated on ice for 30 min, followed by centrifugation at 2000 rpm for 5 min in a Beckman GS-6KR centrifuge. Supernatant was used for determining polyamine content, and pellets were used for protein determination. Protein concentration was determined using the method of Bradford (*25*).

Electrophoretic Mobility Shift Assay (EMSA). EMSA experiments were conducted using breast cancer cellular extracts as previously described (*9*). The duplex NRE was labeled with ^{32}P-γ-ATP using a DNA 5′-end labeling kit from Boehringer Mannheim (Indianapolis, IN). Approximately 30 000−60 000 cpm level of ^{32}P-labeled NRE was mixed with 7.5 μL of cellular extract (∼25 μg of total protein). Prior to the EMSA, polyamines and their analogues were incubated with the radiolabeled oligonucleotide for 1 h at 4 °C. The binding buffer was added to the cellular extract to give a final concentration of 10 mM Tris·HCl, 150 mM KCl, 10% glycerol, 1 mM dithiothreitol, and 10 μg/mL poly(dI−dC)·poly(dI−dC). The NRE-polyamine mixture was added to the cellular extract and the binding reaction allowed to proceed for 1 h at 4 °C, and 30 min at 25 °C, and then loaded on a 5% polyacrylamide gel. Electrophoresis was performed at 200 V for 3 h. The gel was dried and exposed to Kodak Biomax MR-1 film for autoradiography for 24−48 h. Intensity of the DNA−protein band was quantified using a Scanjet flatbed scanner 4c (Hewlett-Packard), and analyzed using NIH Image v1.6 software, using film exposed for <24 h.

Antibody Supershift Assay. To identify the protein−NRE complexes formed in the presence of polyamines, antibodies specific to p50, p65, p52, rel-B, and c-rel were used in the reaction mixture. A supershift of the NF-κB−NRE band or a decrease in the intensity of the band in the presence of

any of the antibodies was considered as an indication of the presence of that protein in the complex.

Transient Transfection assays. MCF-7 cells were used in these experiments. 5×10^5 cells were plated in 35 mm tissue culture dishes and allowed to adhere for 24 h. A 1:1 ratio of pNF-κB−SEAP vector and β-galactosidase (β-gal) control vector were cotransfected using the calcium phosphate mammalian transfection kit (Clontech, Palo Alto, CA), as recommended by the manufacturer. Approximately 2 μg of each plasmid was used for each 35 mm dish. The pNF-κB−SEAP vector contained the secreted alkaline phosphatase reporter gene, with 4 tandem copies of the NF-κB consensus sequence that upon NF-κB binding could induce transcription and activation of the SEAP reporter. The β-galactosidase control vector contained the SV40 promoter and enhancer sequences, and served as a control for normalization of transfection efficiencies. After transfection, cells were allowed to grow in regular medium for 24 h, and then dosed in triplicates with 0.5 mM spermine and assayed for SEAP activity at 6 and 8 h using Great Escape SEAP detection kit, as recommended by the manufacturer (Clontech, Palo Alto, CA). At 8 h, cells were also harvested using PBS and cell pellets processed for β-gal assay using the Luminescent β-gal detection kit. SEAP and luminescent β-gal activity were detected using a tube Luminometer TD-20/20 (Promega, Madison, WI). Light signals were recorded as 10 s integrals. SEAP reporter activity was normalized for each sample using the following equation:

Normalized SEAP Activity = Observed SEAP activity/β-Galactosidase Activity.

In separate experiments, an NF-κB−d2EGFP vector (Clontech, Palo Alto, CA) was transfected into MCF-7 cells; 3×10^4 cells were plated in glass coverslip chambers (Nunc, Naperville, IL) and allowed to adhere for 48 h. Transfection was done using the calcium phosphate mammalian transfection kit (Clontech, Palo Alto, CA); 24 h after transfection, cells were dosed with 0.5 mM spermine and incubation continued for 6 h. The presence of spermine-activated NF-κB-driven transcription of the green fluorescent protein was visualized using a Nikon Eclipse TE200 Microscope with fluorescence attachment, with an excitation wavelength of 450−490 nm and emission at 515 nm. The images were captured by a "SPOT" Color Digital Camera system with 1315×1033 pixel array, and analyzed with a high-resolution graphics workstation with software supplied by the manufacturer (Nikon).

Circular Dichroism Spectroscopy. The CD spectra were recorded on an AVIV model 62D circular dichroism spectrophotometer (AVIV Associates, Lakewood, NJ). All the experiments were performed at 25 °C in rectangular quartz cuvettes of 1 cm path length. The CD spectra were normalized by subtraction of the CD contribution from the buffer. The molar ellipticity was calculated using the equation: $[\theta] = \theta/(cl \times 10)$ where θ is the observed ellipticity, c is the molar concentration of the nucleotide, and l is the path length in centimeters. The molar ellipticity is expressed in terms of deg cm^2 dmol^{-1}. Control experiments showed that none of the polyamines had measurable CD spectral characteristics.

Melting Temperature Measurements. The T_m studies were carried out using a Beckmann DU640 spectrophotometer interfaced with an IBM computer (*21*). The T_m block consists of six cells, each with a volume of ~0.35 mL, of which the first was filled with buffer and used as the blank. All the measurements were done at a heating rate of 0.5 °C min^{-1} using a Beckman high-performance temperature controller, with the absorbance and temperature recorded every 30 s. The T_m measurements were carried out in 10 mM Tris (pH 7.5), containing 50 mM NaCl, and various concentrations of polyamines. T_m was taken as the temperature corresponding to half-dissociation of the duplex and the reproducibility was within 1 °C between individual experiments. The first derivative, dA/dT (where A is the absorbance and T is the temperature) of the melting curve was computer generated and was also used for determining the T_m.

In control experiments, we determined the melting profile of c-NRE in the presence of increasing concentrations of spermine.

High-Performance Liquid Chromatography (HPLC). Polyamine levels of MCF-7 cells treated with spermine were quantified by a previously described procedure (*3*) using a Perkin- Elmer 250 HPLC unit coupled with a Perkin- Elmer LS 40 fluorescence detector. The polyamines were converted to the corresponding dansyl derivatives and separated on a C18 analytical column by eluting with an acetonitrile/water gradient. 1,6-Diaminohexane was used as the internal standard. Polyamine levels are expressed as nmol/mg protein. All experiments were repeated 2−5 times and representative data are presented.

RESULTS

Effect of the Natural Polyamines on NF-κB−NRE Binding. Figure 2 shows the results of a representative EMSA experiment in which cellular extract from MCF-7 cells was incubated with ^{32}P-labeled NRE-1 in the presence of increasing concentrations of spermine, spermidine, or putrescine. There was very little constitutive NF-κB−NRE binding in the cellular extracts of MCF-7 cells. However, spermine facilitated binding at all concentrations tested, with a 5-fold increase in binding at 0.5 mM, as determined by densitometric scanning of the autoradiogram. The maximum increase in binding was 6-fold and leveled off at 1 mM spermine concentration. Spermidine facilitated NF-κB−NRE binding ~ 3.5-fold at 2 mM concentration, and putrescine exerted an approximately 2-fold increase in NF-κB activation at 2 mM concentration. Thus, polyamines are capable of facilitating the binding of NF-κB with its response element, with the following order of efficacy: spermine > spermidine > putrescine.

Since our general experimental design consisted of incubating polyamines with DNA, the polyamine effects may be a consequence of structural/conformational changes of NRE in the presence of polyamines. Therefore, in the next set of experiments, we examined the effects of incubating cellular extracts with spermine, followed by addition of the DNA probe. MCF-7 cellular extract was incubated with increasing concentrations of spermine for 1 h prior to incubation with the ^{32}P-labeled NRE for an additional 1 h at 4 °C and 30 min at 25 °C. As seen in Figure 3, spermine treatment of cellular extract also resulted in a concentration dependent increase in NF-κB−NRE binding, with an approximately 2.5-fold increase at 0.5 mM spermine concentration. The observation of increased binding with spermine

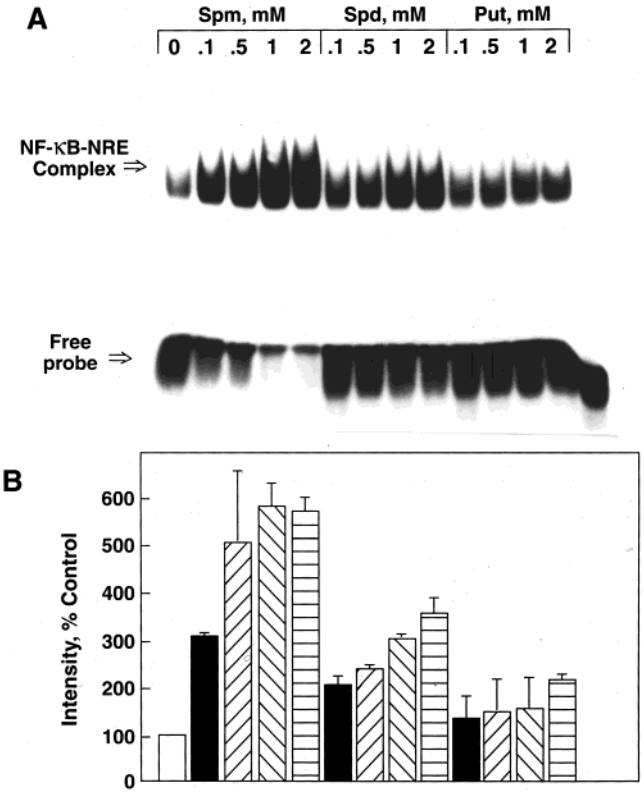

FIGURE 2: Effect of the natural polyamines on NF-κB−NRE interactions using extract from MCF-7 cells. (A) EMSA was conducted using cellular extract and ^{32}P-labeled NRE in the presence of increasing concentrations of either spermine (Spm), spermidine (Spd), or putrescine (Put). The last lane was loaded with free probe (labeled NRE without extract). The reaction mixture was then loaded on a 6% polyacrylamide gel, electrophoresed and autoradiographed. (B) Relative intensities of the NF-κB−NRE complexes in the presence of polyamines as compared to control (100%), as determined by densitometric scanning of the autoradiogram. Average values from two separate experiments are given with error bars.

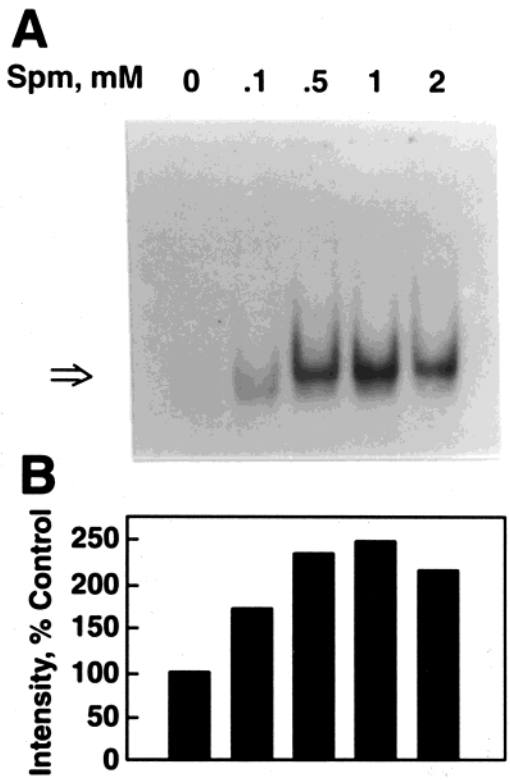

FIGURE 3: Effect of incubating spermine with MCF-7 cellular extract on NF-κB−NRE binding. (A) EMSA was conducted using cellular extract incubated with increasing concentrations of spermine (Spm) for 1 h at 4 °C followed by incubation with ^{32}P-labeled NRE. Arrow represents the NF-κB−NRE complex. (B) Relative intensity of the NF-κB−NRE complexes in the presence of spermine as compared to control (100%), as determined by densitometric scanning of the autoradiogram.

addition in the cellular extract suggests that spermine might act on the protein components of the reaction mixture, although a redistribution of polyamines to NRE during the second incubation cannot be ruled out.

We next examined the effects of spermine on the interaction of NF-κB from the cellular extracts of several breast cancer cell lines with NRE to determine if spermine action on NF-κB−NRE binding was cell specific. Figure 4 shows the results of an EMSA experiment in which cellular extracts from MCF-7, MCF-10AE^{wt5}, MDA-MB-231, MDA-MB-468, SK−BR-3, and MCF-10A cells were incubated with ^{32}P-labeled NRE-1 in the absence or presence of 1 mM spermine. Constitutive NF-κB−NRE binding was significantly higher (3.8−5.6-fold) in all cell lines tested as compared to MCF-7 cells. Spermine caused a 6-fold induction of NF-κB−NRE binding in MCF-7 cells as compared to 1.25-, 1.75-, 1.8-, 2.2-, and 1.65- fold induction in MCF-10AE^{wt5}, MDA-MB-231, MDA-MB-468, SK−BR-3, and MCF-10A cell lines, respectively. This result suggests that factors present in the cellular extract have a role in spermine-induced activation of NF-κB binding to NRE. However, the band intensities of the NF-κB−NRE complexes in the presence of spermine were comparable in all cell lines. Thus, DNA binding affinity may be a limiting factor in the extent of binding observed.

To examine the possible occurrence of spermine-induced activation of NF-κB under conditions of intracellular polyamine accumulation, we treated MCF-7 cells in culture with increasing concentrations of spermine for 6 h prior to harvest. In these experiments, 1 mM aminoguanidine was also added in cell culture to inhibit the activity of amine oxidases. In contrast to previous experiments, no additional spermine was added to the NRE during the EMSA. As shown in Figure 5, spermine treatment of cells activated NF-κB at all concentrations tested, with an ∼2-fold increase in NF-κB−NRE binding at 0.5 mM concentration. Aminoguanidine treatment alone had no effect on NF-κB−NRE binding.

We next performed HPLC analysis to measure intracellular polyamine levels in cells treated with spermine for 6 h, to determine if these levels correlated to the increased NF-κB−NRE binding observed in treated cells. As shown in Table 1, treatment of cells with 2 mM spermine resulted in a 1.7-fold increase in intracellular spermine levels as compared to controls. At this time point, spermidine levels were reduced to 73%, and putrescine levels to 31% of the control. Our results demonstrate that an increase in intracellular spermine concentration in cancer cells can lead to activation of NF-κB.

In the next set of experiments, we questioned whether the facilitating effect of spermine on NF-κB−NRE binding is specific to the NRE1 sequence. We used three other NRE sequences (NRE-2, 3, and 4), that are found in the κ light chain enhancer in B cells, in the promoter region of iNOS,

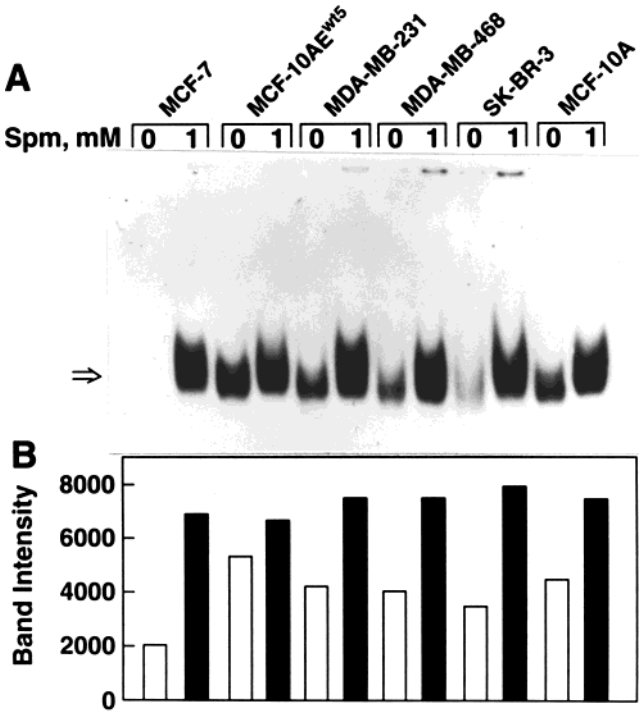

FIGURE 4: Effect of spermine on NF-κB−NRE binding using cellular extract from ER-positive, and ER-negative breast epithelial and cancer cell lines. (A) Cellular extract from MCF-7, MCF-10AE^{wt}5, MDA-MB-231, MDA-MB-468, SK−BR-3, and MCF-10A cells was incubated with ^{32}P-labeled NRE either in the absence or presence of 1 mM spermine (Spm). Arrow represents NF-κB−NRE complex. (B) Intensity of the NF-κB−NRE complexes in arbitrary units, as determined by densitometric scanning of the autoradiogram.

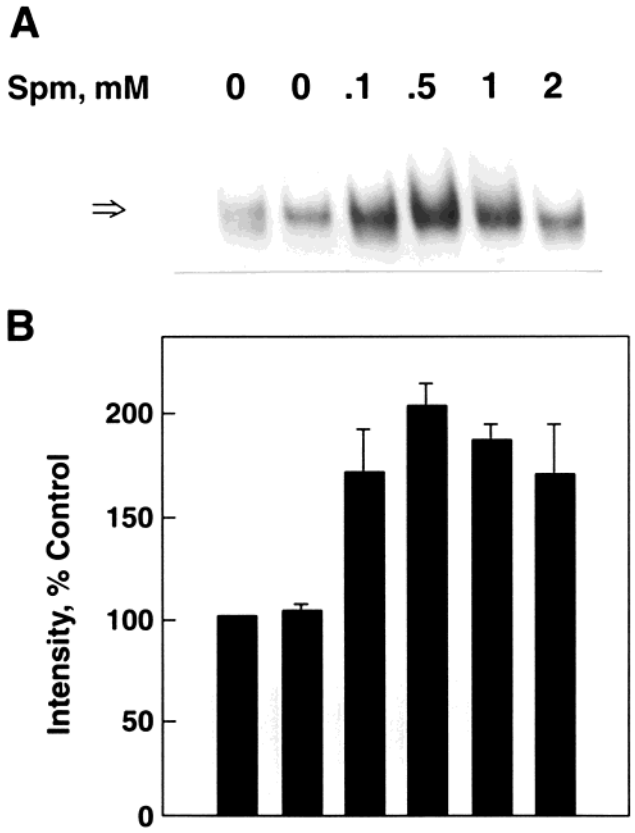

FIGURE 5: Effect of spermine treatment of MCF-7 cells in culture on NF-κB activation. (A) EMSA was conducted using cellular extracts of MCF-7 cells treated with increasing concentrations of spermine for 6 h prior to harvest. Cellular extract was incubated with ^{32}P-labeled NRE for 1 h at 4 °C and 30 min at 25 °C. Arrow represents the NF-κB−NRE complex. First lane represents extract from untreated cells, and second lane represents extract from aminoguanidine treated cells. (B) Relative intensity of the NF-κB−NRE complexes from spermine treated cells as compared to control (100%), as determined by densitometric scanning of the autoradiogram. The average values from two separate treatments are shown with error bars.

and in the promoter region of COX-2 genes, respectively. As shown in Figure 6, spermine facilitated the binding of NF-κB to all these NRE sequences; however, the maximal effect was observed with the consensus NRE. NF-κB−NRE−1 binding was approximately 2-, 2-, and 4-fold higher in the presence of spermine, as compared to that with NRE-2, NRE-3, and NRE-4, respectively.

Characterization of NF-κB−NRE Complex Using Competition with Unlabeled NRE, and Antibodies Specific to Rel Proteins. To determine the specificity of increased NF-κB−NRE binding in the presence of spermine, we performed EMSA experiments in the presence of excess unlabeled oligonucleotide with the wild-type NRE sequence, NRE-1, and a mutated NRE sequence, *m*-NRE. Figure 7 shows the results of the competition experiments. At 5X concentration of wild-type unlabeled NRE-1, complete inhibition of NF-κB binding to the labeled NRE-1 was found. In contrast, even at 100X concentration, *m*-NRE was not able to completely inhibit NF-κB binding to labeled NRE-1. This result shows the sequence specificity of NF-κB-binding to DNA.

To identify the proteins recruited to bind to NRE in the presence of polyamines, EMSA was performed using MCF-7 cellular extract incubated with ^{32}P-labeled NRE-1 and either 0.1 or 1 mM spermine, and 2 μg of either p50, p65, p52, rel-B, or c-rel antibodies. The protein−DNA band was supershifted only in the presence of p50 antibody showing that the enhanced binding from breast cancer cellular extracts in the presence of polyamines was mainly due to the binding of p50 (Figure 8). However, there was a 30−35% reduction in the intensity of the NF-κB−NRE complex band in the presence of anti-p65 and anti-c-rel antibodies, and a 15−20% reduction in the presence of anti-p52 and anti rel-B antibodies, suggesting the possible involvement of these proteins also in complex formation.

We also performed antibody supershift experiments using MCF-7 cellular extract incubated with ^{32}P-labeled NREs-2, 3, and 4, using antibodies to p50 and p65 proteins in order

Table 1: Polyamine Levels in MCF-7 Cells Treated with Spermine in Culture

treatment/concentration, mM		intracellular polyamine concentrations, nmole/mg protein[a]		
aminoguanidine[b]	spermine	putrescine	spermidine	spermine
0	0	0.85 ± 0.02	7.85 ± 0.35	7.37 ± 0.01
1	0	0.76 ± 0.01	8.97 ± 0.39	8.18 ± 0.16
1	0.25	0.26 ± 0.04	6.34 ± 0.44	10.85 ± 0.23
1	0.5	0.26 ± 0.01	6.41 ± 0.13	11.83 ± 0.15
1	1	0.23 ± 0.004	5.87 ± 0.21	11.88 ± 0.08
1	2	0.27 ± 0.01	5.77 ± 0.14	12.41 ± 0.35

[a] Polyamine levels were quantified by HPLC technique from cells treated with spermine for 6 h. Data presented are the mean± S.D. of triplicate measurements. [b] Cells were treated with the indicated concentrations of aminoguanidine and spermine. Aminoguanidine was used to inhibit the action of polyamine oxidase.

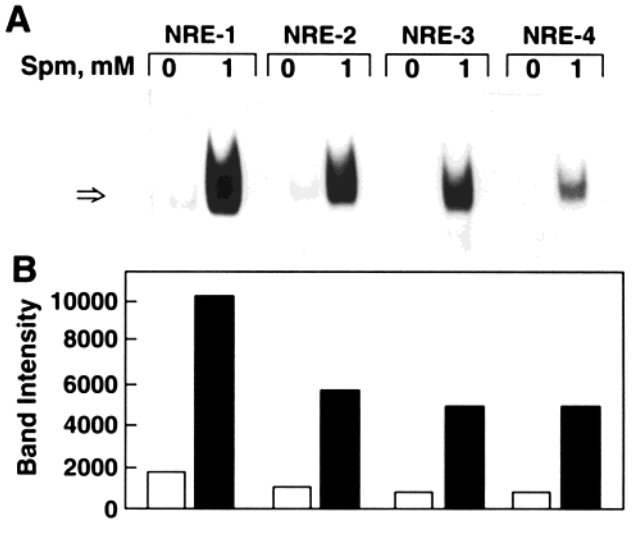

FIGURE 6: Effect of NRE sequence on spermine-mediated NF-κB−NRE binding. (A) EMSA was conducted using cellular extract from MCF-7 and ^{32}P-labeled NRE-1, NRE-2, NRE-3 and NRE-4, either in the absence or presence of 1 mM spermine (Spm). Arrow represents the NF-κB−NRE complex. (B) Intensity of the NF-κB−NRE complexes in arbitrary units, as determined by densitometric scanning of the autoradiogram.

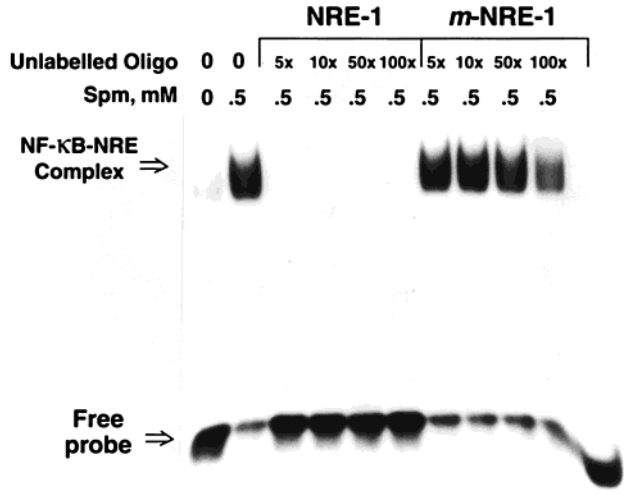

FIGURE 7: Determination of specificity of NF-κB−NRE binding. EMSA was conducted with MCF-7 cellular extract incubated with ^{32}P-labeled NRE in the absence or presence of 1 mM spermine (Spm). Increasing concentrations of unlabeled NRE-1 or *m*-NRE-1 was incubated with the ^{32}P-labeled NRE-1 in the presence of spermine for 1 h prior to addition of the cellular extract.

to characterize the protein−DNA bands. In each case, the protein−NRE band was supershifted only in the presence of the p50 antibody. However, there was a 35% reduction in the intensity of the NF-κB−NRE complex band in the presence of anti-p65 antibody, suggesting the participation of the p65 subunit also in complex formation in the presence of spermine. We found comparable results with all 4 NRE sequences tested (results not shown).

Differential Effects of Polyamine Analogues on NF-κB−NRE Binding. To examine the structural specificity effects of polyamines on modulating NF-κB−NRE interactions, we used a series of spermine analogues, $NH_2(CH_2)_3NH(CH_2)_n$-$NH(CH_2)_3NH_2$ (where $n = 2-9$; $n = 4$ for spermine). Figure 9A shows that spermine had the maximum stimulatory effect on NF-κB−NRE binding and the analogue 3-2-3 had the least effect. Binding in the presence of the other analogues was 4- to 5-fold higher than that of the control. The effect of 3-2-3 may be partially due to its reduced protonation at a buffer pH of 7.4. The reduced effect of the higher homologues in inducing NF-κB−NRE binding, as compared to spermine, reflects the structural specificity effects of polyamines. However, these analogues did not show dramatic differences in facilitating NF-κB−NRE interaction.

We also conducted EMSA experiments using a series of spermidine analogues, $NH_2(CH_2)_3NH(CH_2)_nNH_2$ (where $n = 2-8$; $n = 4$ for spermidine). As shown in Figure 9B, the analogues with $n = 3$, 5, and 7, i.e., an odd number of methylene groups, enhanced NF-κB−NRE binding as compared to the preceding analogue, i.e., the analogues with $n = 2$, 4, 6, or 8, respectively. The differential efficacy of spermidine analogues in stimulating NF-κB−NRE interaction

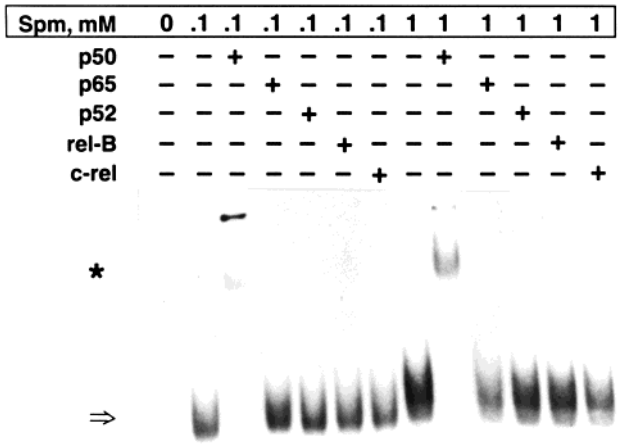

FIGURE 8: Characterization of the protein-NRE band using antibody supershift assay. EMSA was conducted using MCF-7 cellular extract incubated with ^{32}P-labeled NRE-1 in the absence or presence of 1 mM spermine (Spm) with 2 μg of either anti-p50, p65, p52, rel-B or c-rel antibodies. An arrow represents the protein−DNA complex, and asterisk represents the p50−NRE complex with anti-p50, as it is supershifted in the presence of the p50 antibody.

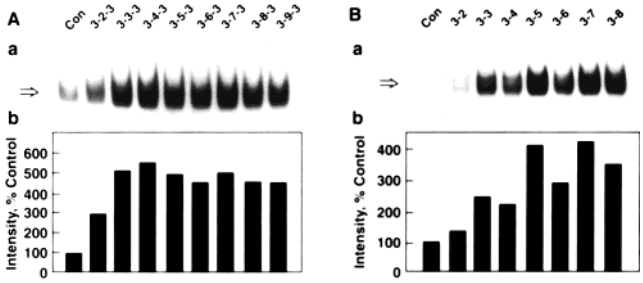

FIGURE 9: (A) Effect of spermine analogues on NF-κB−NRE interactions. (a) EMSA was conducted using cellular extract from MCF-7 cells and ^{32}P-labeled NRE in the presence of 0.5 mM spermine analogues. Con represents control (cellular extract with 20 000 cpm of labeled NRE). An arrow represents the NF-κB-NRE complex. (b) Relative intensity of the NF-κB−NRE complex in the presence of spermine analogues, as compared to the control (100%), as determined by densitometric scanning of the autoradiogram. (B) Effect of spermidine analogues on NF-κB−NRE interaction using extract from MCF-7 cells. (a) EMSA was conducted with cellular extract incubated and ^{32}P-labeled NRE in the presence of 1 mM spermidine analogues. Con represents control (cellular extract with 20 000 cpm of labeled NRE). An arrow represents the NF-κB−NRE complex. (b) Relative intensity of the NF-κB−NRE complex in the presence of spermidine analogues, as compared to the control (100%), as determined by densitometric scanning of the autoradiogram.

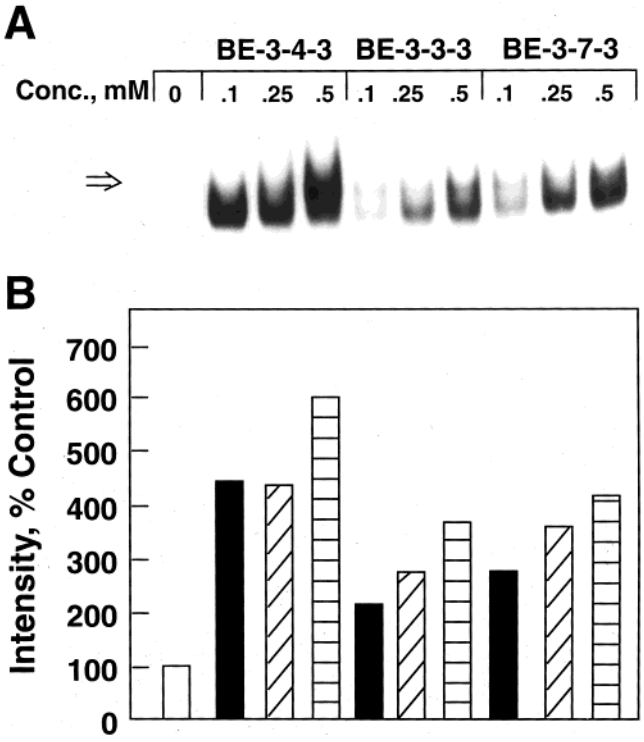

FIGURE 10: Effect of bis(ethyl) spermine analogues on NF-κB−NRE binding. (A) EMSA was conducted using cellular extract from MCF-7 cells with ^{32}P-labeled NRE in the presence of increasing concentrations of BE-3-4-3, BE-3-3-3, and BE-3-7-3. An Arrow represents the NF-κB−NRE complex. (B) Relative intensity of the NF-κB−NRE complex in the presence of the bis(ethylated) spermine analogues, as compared to the control (100%), as determined by densitometric scanning of the autoradiogram.

shows that not only the charge, but also the number of methylene groups between the primary and secondary amino groups plays an important role in the function of polyamines.

Bis(ethyl)polyamine analogues are currently emerging as a novel class of experimental chemotherapeutic agents (*26*). We conducted EMSA in which MCF-7 cellular extract was incubated with ^{32}P-labeled NRE-1 in the presence of increasing concentrations of BE-3-4-3, BE-3-3-3, and BE-3-7-3. As shown in Figure 10, BE-3-4-3 had a similar effect as spermine in inducing NF-κB−NRE binding, with a 6-fold increase in binding at 0.5 mM concentration. BE-3-3-3 and BE-3-7-3 were significantly less effective than spermine in activating NF-κB−NRE binding.

To differentiate between ionic and structural specificity effects of polyamines, and to test if the charge distribution of polyamines is in part responsible for their effects on protein−DNA interaction, we performed EMSA using the inorganic polycations Mg^{2+} and $Co(NH_3)_6^{3+}$. As shown in Figure 11, 2 mM $Co(NH_3)_6^{3+}$ and 5 mM Mg^{2+} stimulated NF-κB−NRE binding by 3- and 2-fold, respectively. These concentrations of $Co(NH_3)_6^{3+}$ and Mg^{2+}, are 4- and 10-fold higher than that of spermine (0.5 mM), respectively, in facilitating NF-κB−NRE interaction. These results demonstrate that inorganic cations are much less efficacious in activating NF-κB−NRE binding, indicating the importance of polyamine structure in this interaction.

T_m and CD Spectral Studies of NRE in the Presence of Spermine. To test the conformational and structural alterations of NRE in the presence of spermine, we conducted T_m and CD spectral studies. Figure 12 shows the CD spectra

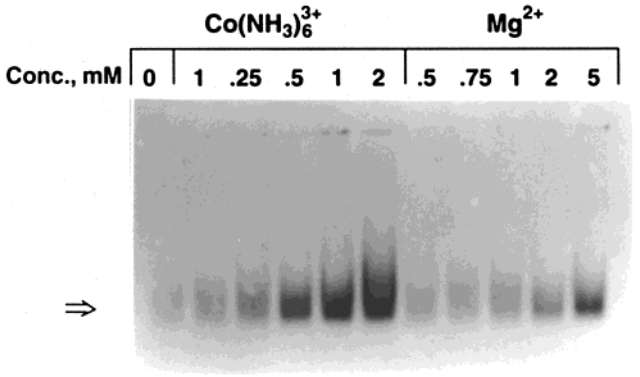

FIGURE 11: Effect of inorganic cations on NF-κB−NRE binding. EMSA was conducted using cellular extract from MCF-7 cells incubated with ^{32}P-labeled NRE in the presence of increasing concentrations of Mg^{2+} and Co(NH3)3^{6+}. Arrow represents the NF-κB−NRE complex.

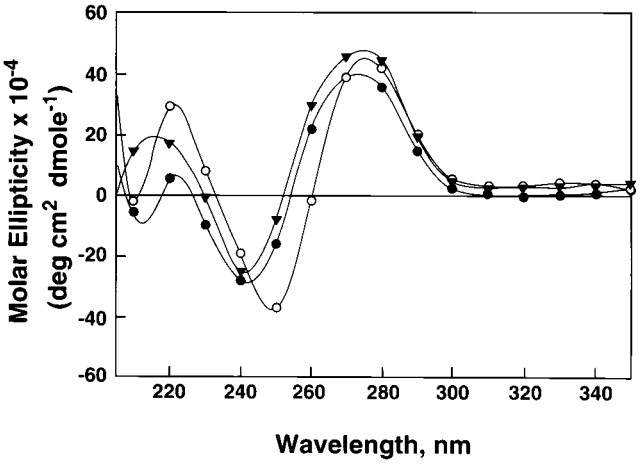

FIGURE 12: CD spectra of c-NRE, NRE-1, and NRE-4. CD spectra of the oligonucleotides was recorded in a buffer containing 10 mM Tris (pH 7.4) and 50 mM NaCl. Symbols represent c-NRE (○), NRE-1 (●) and NRE−4 (▼).

of the c-NRE, NRE-1, and NRE-4 in 10 mM Tris (pH 7.4), containing 50 mM NaCl. The shape of the CD spectrum of the c-NRE is characteristic of B-DNA, with conservative positive and negative bands at 270 and 250 nm, respectively, and a positive band at 220 nm. The CD spectrum of NRE-1 and NRE-4 shows a broad positive band centered at 270 nm similar to those found in A-DNA. However, the negative band found at 240 nm is more intense than that found for A-DNA. In addition, NRE-1 and NRE-4 showed bands with less intensity than c-NRE in the 215−220 nm region. Thus, the CD spectra of NRE-1 and NRE-4 are indicative of a structural intermediate between the A-DNA and B-DNA. The CD spectra of the oligonucleotides in the presence and absence of polyamines were not significantly different (results not shown). These results show a sequence-dependent conformational plasticity of NRE oligonucleotides; however, further conformational transitions were not detected in the presence of polyamines.

Our T_m analysis indicated an increase in the stability of NRE in the presence of all polyamines. As shown in Table 2, the efficacy of polyamines in increasing T_m was in the order: spermine > spermidine > putrescine. T_m of NRE-1 in the presence of spermine was 13 °C higher than that of NRE-1 alone. These results indicate that polyamines stabilize the NRE oligonucleotide duplexes, thus making them more

Table 2: Effect of Natural Polyamines on the T_m of NRE-1 and c-NRE

polyamine	concentration, mm	melting temperature, °C[a]	
		NRE-1	c-NRE
putrescine	0	70.6	N.D.[b]
	0.25	70.9	N.D.
	0.5	71.8	N.D.
	1.0	73.7	N.D.
	2.0	75.7	N.D.
spermidine	0	70.7	N.D.
	0.1	72.7	N.D.
	0.25	72.7	N.D.
	0.5	77.7	N.D.
	1.0	79.7	N.D.
	2.0	81.5	N.D.
spermine	0	70.8	72.9
	0.1	79.7	79.8
	0.25	81.9	81.8
	0.5	81.9	81.8
	1.0	83.8	83.8
	2	83.8	84.7

[a] T_m measurements were done by recording absorbance−temperature profile at a heating rate of 0.5 °C/min in a buffer containing 10 mM Tris (pH 7.5) and 50 mM NaCl. [b] N.D. Not determined.

conducive to protein binding. However, this effect was present in cNRE as well as NRE-4, which showed the least increase in NF-κB−NRE binding. Polyamines have been shown to stabilize duplex and triplex DNA by dramatically increasing their T_m (*19*, *27*).

To test if the spermine-induced activation of NF-κB−NRE binding in vitro corresponds to transcriptional activation in the cell, we performed transient transfection experiments using an NF-κB driven SEAP reporter plasmid. A β-gal control vector was used to normalize for transfection efficiencies. As shown in Figure 13, spermine treatment resulted in an ∼2-fold induction of the transcriptional activity of NF-κB as compared to controls.

We also performed transfection experiments using an NF-κB driven EGFP reporter. As seen in Figure 14, treatment with spermine caused a greater induction of the green fluorescent protein as compared to controls. Figure 14 also shows the same set of MCF-7 cells using both phase contrast and fluorescence microscopy for the control and spermine-treated cells. These results further confirm that spermine-induced increases in NF-κB−NRE binding result in transcriptional activation of NF-κB.

DISCUSSION

Our results show that the natural polyamine, spermine, exerts a significant stimulatory effect on NF-κB−NRE binding in breast cancer cells. Spermidine and putrescine are also capable of facilitating NF-κB−NRE binding, but to a lesser extent as compared to spermine, and at higher concentrations. This could be partially attributable to the higher cationicity of spermine (4^+) as compared to spermidine (3^+) and putrescine (2^+). In addition to cationicity, the structure of the natural polyamines appears important, since Mg^{2+} was 2-fold less effective than putrescine in inducing NF-κB−NRE binding. Polyamine analogues, BE-3-3-3 (4^+) and BE-3-7-3 (4^+) were less effective than spermine in facilitating NF-κB−NRE binding. These results suggest that certain polyamine analogues may inhibit spermine-induced NF-κB−NRE binding.

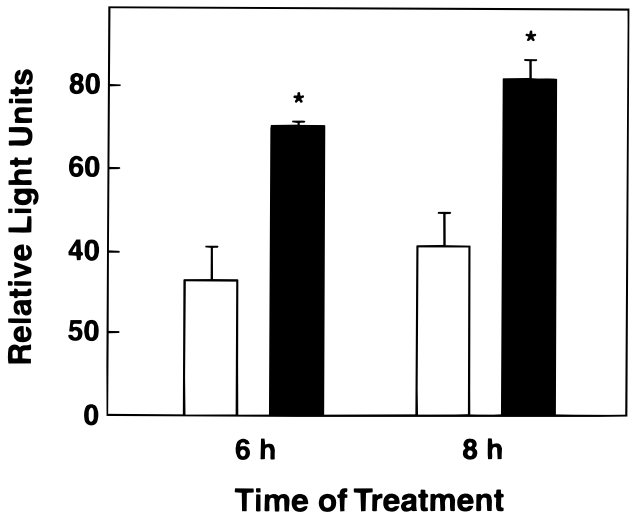

FIGURE 13: Effect of spermine on NF-κB-mediated transcriptional activation of SEAP reporter gene. Plasmids, pNF-κB−SEAP, and β-galactosidase control vector were cotransfected in MCF-7 cells. Cells were treated with 0.5 mM spermine 24 h after transfection. Media was assayed at 6 and 8 h of spermine treatment for the presence of SEAP. SEAP reporter activity is expressed as relative light units and was normalized for each sample using the following equation: Normalized SEAP activity = Observed SEAP activity/β-galactosidase activity. Untreated control (□) and 0.5 mM spermine treatment (■) groups are shown. Data represents average from triplicate measurements and represents significance at $p < 0.025$, as determined by the Student's t-test.

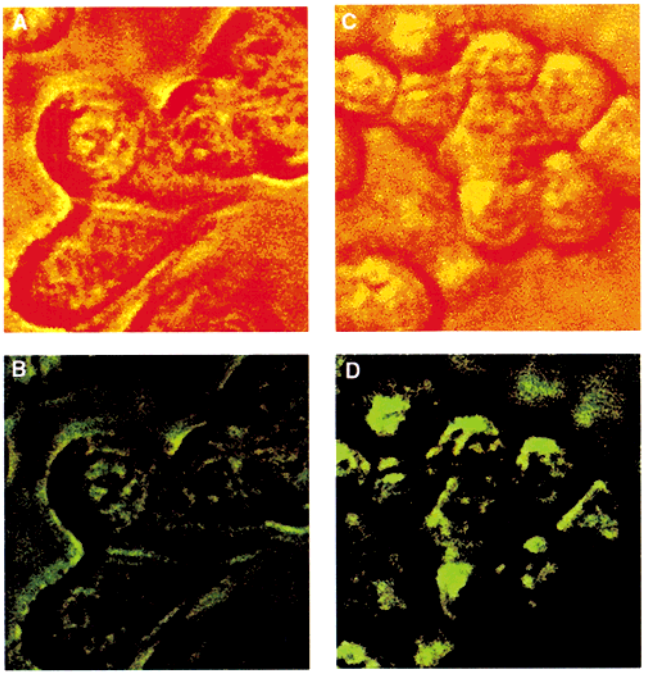

FIGURE 14: Effect of spermine on NF-κB driven EGFP expression. MCF-7 cells were transfected with a plasmid containing an NF-κB driven EGFP reporter. Cells were allowed to proliferate for 24 h after which 0.5 mM spermine was added and cells incubated for an additional 6 h. The synthesis of EGFP was visualized using fluorescence microscopy. A and C represents control and spermine-treated cells, respectively, observed using phase-contrast microscopy. B and D represents the same set of cells observed using fluorescence microscopy.

Spermine had the maximum stimulatory effect on NF-κB−NRE binding and the spermine analogue 3-2-3 had the least effect. Binding in the presence of the other analogues ranged

between those of spermine and 3-2-3. The effect of 3-2-3 may be partially due to its reduced protonation at a buffer pH of 7.4. For example, 3-2-3 has reported pK_a values of 10.7, 10.0, 8.5, and 5.8, suggesting that at pH 7.4, i.e., at the conditions of our experiment, this molecule might act as a triamine (*28*). In contrast, spermine has pK_a values of 10.9, 10.1, 8.8, and 7.9 (*29*). The higher homologues of spermine, due to the increased charge separation, have pK_a values close to or higher than that of spermine (*28*, *29*). Excepting 3-2-3, the other analogues did not show dramatic differences in facilitating NF-κB−NRE binding. The bisethylated analogue, BE-3-4-3, also had a similar effect on NF-κB−NRE binding as spermine. These data indicate that either a change in methylene length, or substitution at the pendant amino groups alone is not sufficient to diminish the polyamine effects exerted by an analogue; however, a combination of both these alterations, as in BE-3-3-3, can reduce the ability of polyamines to activate NF-κB.

Spermidine analogues with 3, 5, and 7 methylene bridging groups between the primary and secondary amino groups enhanced NF-κB−NRE binding. In contrast, the analogues with 2, 4 (spermidine), 6, or 8 methylene groups were less effective than their preceding homologues in enhancing NF-κB−NRE interaction, although there was an increase in binding with increasing chain length. Diaminoalkanes with an odd number of carbon atoms have been shown to induce compaction of DNA molecules in contrast to the diaminoalkanes with an even number of carbon atoms (*30*), suggesting a possible mode of action of spermidine homologues in NF-κB−NRE interaction.

We found a 4-fold lower binding of NF-κB to NRE-4 as compared to NRE-1, in the presence of spermine. T_m results indicate a similar stabilization effect of spermine on both NRE-1, and NRE-4. Thus, this difference in binding cannot be attributed to differential stabilization of the NRE duplex. However, the effects of differential binding of polyamines to different NRE sequences or microstructural alterations of the NRE sequences cannot be ruled out at present. The p50 homodimer has been shown to bind with high affinity to a palindromic enhancer sequence, whereas NRE sequences having reduced symmetry are bound preferentially by the p50−p65 heterodimer (*31*). Since the major component in our experiments seems to be p50 binding, this would help explain the highest binding seen with NRE-1, a palindromic sequence, and lower levels of binding seen with NREs-2, -3, and -4, which are imperfect palindromes.

DNA bending has been suggested to be important for NF-κB−DNA recognition (*31*). Binding of purified NF-κB to DNA induces strong DNA bending that can facilitate the interaction between proteins bound to separate sites on DNA. NF-κB−DNA binding has been shown to be facilitated by spermine and certain cations (*30*), which are known to promote DNA bending.

It is postulated that polyamines, by neutralizing charges on DNA, reduce the energy requirement for bending and thus facilitate enhanced protein−DNA interaction. Recently, Rouzina and Bloomfield (*32*) proposed a mechanism by which small multivalent cations induce DNA bending by binding at the entrance to the B-DNA major groove between the two phosphate strands, thus repelling sodium counterions from the neighboring phosphates, which then get strongly attracted to the groove bound cations leading to groove closure and DNA bending around the cationic ligand. If in fact, NRE bending by polyamines is involved in facilitation of NF-κB−NRE binding, such a mechanism of DNA bending would help explain the decreased efficacy of the bis-ethylated polyamine analogues (BE-3-3-3 and BE-3-7-3) in facilitating NF-κB−NRE binding, since they may not be as mobile and efficient as the natural polyamines in interacting with DNA due to steric hindrance caused by their bulky ethyl groups.

Several modes of polyamine binding to DNA have been proposed, besides the electrostatic interaction between the positive charges on the polyamines and the negative phosphate charges on the DNA (*33*−*36*). Polyamines have been shown to stabilize unusual structures such as A-DNA, Z-DNA, triplex DNA, and bent DNA (*19*, *37*, *38*). Our CD spectroscopic studies showed a difference in NRE-1 and NRE-4 conformation as compared to a control oligonucleotide that showed a typical B-DNA spectrum. This finding is in agreement with the results of Matthews et al. (*46*), which showed that the CD spectrum of a high-affinity κB motif is asymmetric and unlike that of typical B-form DNA. The CD spectra of the oligonucleotides were not significantly altered by the addition of polyamines, although the T_m data showed a concentration-dependent increase in the stabilization of the duplex. It is thus possible that the effect of spermine on facilitating NF-κB−NRE interaction might be related to the stabilization of secondary/tertiary structures of NRE. Previous studies using CD spectra and chymotrypsin sensitivity have demonstrated that the conformation of p50 protein as well as that of the NRE duplex DNA were changed when p50 was bound to the fully symmetrical high affinity NRE, but not with less tightly bound DNA (*39*). Thus, polyamines may facilitate NF-κB−NRE complex formation, even though no drastic changes were seen in the CD spectrum of the oligonucleotides in the presence of spermine.

Polyamines have been shown to enhance the binding of several proteins to DNA (9, *10*, *40*). In addition, the reduction of polyamine levels in cells by polyamine oxidase treatment has been shown to decrease the DNA binding activity of the transcription factors NFAT, and NF-κB (*41*). In EMSA experiments, we found very little constitutive NF-κB-DNA binding activity in the ER-positive MCF-7 cells. In previous studies of NF-κB-DNA binding activity of breast cancer cell lines and tissues, different levels of binding were observed (*16*). Transient transfection analysis using the upstream regulatory element of an NF-κB responsive gene demonstrated that constitutive DNA binding activity was functionally active (*16*). In a similar approach, we examined the expression of genes linked to NF-κB response element in the presence and absence of spermine. Our results, using SEAP as well as EGFP reporter genes, confirmed that spermine is capable of functionally activating NF-κB.

In our antibody supershift experiments, only p50 showed a shifted band consisting of the protein−DNA complex and the antibody, although decreases in NF-κB−NRE complexes were found in the presence of other Rel antibodies. It is thus possible that p50 homodimers, or heterodimers including other Rel transcription factors, may be involved in the observed increase in NF-κB−NRE binding. Since p50 homodimer does not have the transactivation domain, it is assumed to repress transcription by competing for binding sites (*42*). However, there is conflicting evidence as to the role of p50 homodimers in mediating transcription. p50

homodimers either inhibit or stimulate gene expression depending on the presence of other coregulatory proteins. Overexpression of p50 has been shown to block lipopolysaccharide-induced transcription from a TNF-α promoter reporter construct (*43*) as well as block p65-mediated transcription of ICAM-1 promoter reporter construct (*44*). In contrast, the nuclear cofactor bcl-3 has been shown to superactivate NF-κB p50 homodimer-mediated gene expression both in vivo and in vitro by forming a transcription-activating ternary complex with p50 (*45*). The high mobility group protein (HMG-I (Y)) has also been shown to be involved in the formation of a ternary complex containing itself, p50, and the iNOS promoter/enhancer as well as to increase iNOS activity in the presence of p50, although to a lesser extent than when transfected with both p50 and p65 (*46*). Thus, p50 activation would have differential effects, depending on the micro-environment of the cell and the presence of accessory proteins. Since polyamines and NF-κB are overexpressed in breast tumors and cancer cell lines, a concerted action of these agents might play a role in growth-related gene activation, especially those containing NRE sequences, such as COX-2 and iNOS genes.

Our results suggest that multiple pathways contribute to polyamine-mediated activation of NF-κB−NRE binding. These factors include duplex stabilization, bending, and interactions of polyamines with the protein, DNA, and/or the protein−DNA complex. Different aspects of the natural polyamines (i.e., cationicity, structure, and function in the cell) seem to be important to varying degrees in these functions, as seen by the effects of the polyamine analogues (differing in cationicity, methylene bridging of the amino and imino groups, and presence of additional ethyl groups) in substituting for natural polyamines in NF-κB activation.

CONCLUSIONS

Several conclusions can be drawn from the data presented in this paper: (i) spermine is the most potent natural polyamine in inducing NF-κB−NRE binding; (ii) tetramines enhance NF-κB−NRE binding better than triamines (spermine analogues vs spermidine analogues); (iii) inorganic cations such as $MgCl_2$ are less effective than spermine in inducing NF-κB−NRE binding; (iv) spermidine analogues with an odd number of methylene groups are more efficient at inducing NF-κB−NRE binding as compared to preceding analogues with an even number of methylene groups (e.g., 3-7 vs 3-6); (v) antibody supershift data demonstrate that one of the proteins induced to bind to the NRE by polyamines is p50, although the participation of other rel-related proteins, especially p65 is also indicated; (vi) BE-3-3-3 is less effective than spermine in activating NF-κB, suggesting that a possible mechanism of action of this therapeutic polyamine analogue might involve its inability to activate NF-κB; (vii) the increase in DNA binding activity of NF-κB observed in the presence of spermine is functionally important in activating NF-κB responsive genes as demonstrated by transient transfection assays.

REFERENCES

1. Pegg, A. E. (1988) *Cancer Res. 48*, 759−774.
2. Tabor, C. W., and Tabor, H. (1984) *Annu. Rev. Biochem. 53*, 749−790.
3. Thomas, T., Faaland, C. A., Adhikarakunnathu, S., and Thomas, T. J. (1996) *Breast Cancer Res. Treat. 39*, 293−306.
4. Leveque, J., Bansard, J. Y., Watier, E., Catros-Quemener, V., Havouis, R., Moulinoux, J. P., Grall, J. Y., Seiler, N. (1999) *Anticancer Res. 19*, 2275−2279.
5. Porter, C. W., McManis, J., Casero, R. A., and Bergeron, R. J. (1987) *Cancer Res. 47*, 2821−2825.
6. Porter, C. W., Herrera-Ornelas, L., Pera, P., Petrelli, N. F., and Mittelman, A. (1997) *Cancer* 60, 1275−1281.
7. Soler, A. P., Gilliard, G., Megosh, L., George, K., and O'Brien, T. G. (1998) *Cancer Res. 58*, 1654−1659.
8. Marton, L. J., and Pegg, A. E. (1995) *Annu. Rev. Pharmacol. Toxicol. 35*, 55−91.
9. Thomas, T., Gallo, M. A., Klinge, C. M., and Thomas, T. J. (1995) *J. Steroid Biochem. Mol. Biol. 54*, 89−99.
10. Wang, Y., Xiao L., Thiagalingam, A., Nelkin, B. D., and Casero, R. A., Jr. (1998) *J. Biol. Chem. 273*, 34623−34630.
11. Baeuerle, P. A., and Baltimore, D. (1988) *Science 242*, 540−546.
12. Boland, M. P., Foster, S. J., and Oneill, L. A. J. (1997) *J. Biol. Chem. 272*, 12952.
13. Das, K. C., and White, C. W. (1997) *J. Biol. Chem. 272*, 14914−14920.
14. Baeuerle, P. A. (1991) *Biochim. Biophys. Acta. 1072*, 63−80.
15. Grassilli, E., Desiderio, M. A, Bellesia, E., Salomoni, P., and Benatti, F., Franceschi, C. (1995) *Biochem. Biophys. Res. Commun. 216*, 708−714.
16. Sovak, M. A., Bellas, R. E., Kim, S. W., Zanieski, G. J., Rogers, A. E., Traish, A. M., and Sonenshein, G. E. (1997) *J. Clin. Invest. 100*, 2952−2960.
17. Nakshatri, H., Bhat-Nakshatri, P., Martin, D. A., Goulet, R. J., Jr., and Sledge, G. W., Jr. (1997) *Mol. Cell Biol. 17*, 3629−39.
18. Wang, C.-Y., Mayo, M. W., and Baldwin, A. S., Jr. (1996) *Science 274*, 784−87.
19. Thomas, T. J., and Bloomfield, V. A. (1984) *Biopolymers 23*, 1295−1306.
20. Musso, M., Thomas, T., Shirahata, A., Sigal, L. H., van Dyke, M. W., and Thomas, T. J. (1997) *Biochemistry 36*, 1441−1449.
21. Antony, T., Thomas, T., Shirahata, A., Sigal, L. H., and Thomas, T. J. (1999) *Antisense Nucleic Acid Drug Dev. 9*, 221−231.
22. He, Y., Suzuki, T., Kashiwagi, K., Kusama-Eguchi, K., Shirahata, A., and Igarashi, K. (1994) *Eur. J. Biochem. 221*, 391−398.
23. Igarashi, K., Koga, K., He, Y., Shimogori, T., Ekimoto, H., Kashiwagi, K., and Shirahata, A. (1995) *Cancer Res. 55*, 2615−2619.
24. Thomas, T. J., Faaland, C. A., Adhikarakunnathu, S., Watkins, L., and Thomas, T. (1998) *Breast Cancer Res. Treat. 47*, 181−193.
25. Bradford, M. M. (1976) *Anal. Biochem. 72*, 248−254.
26. Kramer, D. L., Fogel-Petrovic, M., Diegelman, P., Cooley, J. M., Bernacki, R. J., McManis, J. S., Bergeron, R. J., and Porter, C. W. (1997) *Cancer Res. 57*, 5521−5527.
27. Thomas, T., and Thomas, T. J. (1993) *Biochemistry 32*, 14068−14074.
28. Stewart, K. D., and Gray, T. A. (1992) *J. Phys. Org. Chem. 5*, 461−466.
29. Aikens, D., Bunce, S., Onasch, F., Parker, R., Hurwitz, C., and Clemans, S. (1983) *Biophys. Chem. 17*, 67−74.
30. Schreck, R., Zorbas, H., Winnacker, E. L., and Baeuerle, P. A. (1990) *Nucleic Acids Res. 18*, 6497−6502.
31. Urban, M. B., and Baeuerle, P. A. (1991) *The New Biol. 3*, 279−288.
32. Rouzina, I., and Bloomfield, V. A. (1998) *Biophys. J. 74*, 3152−3164.
33. Zhurkin, V. B., Lysov, Y. P., and Ivanov, V. I. (1980) *Biopolymers 19*, 1415−1428.
34. Egli, M., Williams, L. D., Gao, Q., and Rich, A. (1991) *Biochemistry 30*, 11388−11402.
35. Jain, S., Zon, G., and Sundaralingam, M. (1989) *Biochemistry 28*, 2360−2366.

36. Schmid, N., and Behr, J. P. (1991) *Biochemistry 30*, 4357−4361.
37. Basu, H. S., and Marton, L. J. (1987) *Biochem. J. 244*, 243−246.
38. Thomas, T. J., and Messner, R. P. (1988) *J. Mol. Biol. 201*, 463−467.
39. Matthews, J. R., Nicholson, J., Jaffray, E., Kelly, S. M., Price, N. C., and Hay, R. T. (1995) *Nucleic Acids Res. 23*, 3393−3402.
40. Pangiotidis, C. A., Artandi, S., Calame, K., and Silverstein, S. J. (1995) *Nucleic Acids Res. 23*, 1800−1809.
41. Flescher, E., Ledbetter, J. A., Schieve, G. L., Vela-Roch, N., Fossum, D., Dang, H., Ogawa, N., and Talal, N. (1994) *J. Immunol. 153*, 4880−4889.
42. Liou, H.-C., and Baltimore, D. (1993) *Curr. Opin. Cell. Biol. 5*, 477−487.
43. Baer, M., Dillner, A., Schwartz, R. C., Sedon, C., Nedospasov, S., and Johnson, P. F. (1998) *Mol. Cell. Biol. 18*, 5678−5689.
44. Lee, S. J., Hou, J., and Benveniste, E. N. (1998) *J. Neuroimmunol. 92*, 196−207.
45. Fujita, T., Nolan, G. P., Liou, H. C., Scott, M. L., and Baltimore, D. (1993) *Genes Dev. 7*, 1354−1363.
46. Perrella, M. A., Pellacani, A., Wiesel, P., Chin, M. T., Foster, L. C., Ibanez, M., Hsieh, C−M., Reeves, R., Yet, S.-F., and Lee M−E. (1999) *J. Biol. Chem. 274*, 9045−9052.

BI991291V